ORIGINAL ARTICLE

A Form of the Metabolic Syndrome Associated with Mutations in *DYRK1B*

Ali R. Keramati, M.D., Mohsen Fathzadeh, Ph.D., Gwang-Woong Go, Ph.D., Rajvir Singh, Ph.D., Murim Choi, Ph.D., Saeed Faramarzi, M.D., Shrikant Mane, Ph.D., Mohammad Kasaei, M.D., Kazem Sarajzadeh-Fard, M.D., John Hwa, M.D., Ph.D., Kenneth K. Kidd, Ph.D., Mohammad A. Babaee Bigi, M.D., Reza Malekzadeh, M.D., Adallat Hosseinian, M.D., Masoud Babaei, M.D., Richard P. Lifton, M.D., Ph.D., and Arya Mani, M.D.

ABSTRACT

BACKGROUND

Genetic analysis has been successful in identifying causative mutations for individual cardiovascular risk factors. Success has been more limited in mapping susceptibility genes for clusters of cardiovascular risk traits, such as those in the metabolic syndrome.

METHODS

We identified three large families with coinheritance of early-onset coronary artery disease, central obesity, hypertension, and diabetes. We used linkage analysis and whole-exome sequencing to identify the disease-causing gene.

RESULTS

A founder mutation was identified in *DYRK1B*, substituting cysteine for arginine at position 102 in the highly conserved kinase-like domain. The mutation precisely cosegregated with the clinical syndrome in all the affected family members and was absent in unaffected family members and unrelated controls. Functional characterization of the disease gene revealed that nonmutant protein encoded by *DYRK1B* inhibits the SHH (sonic hedgehog) and Wnt signaling pathways and consequently enhances adipogenesis. Furthermore, DYRK1B promoted the expression of the key gluconeogenic enzyme glucose-6-phosphatase. The R102C allele showed gain-of-function activities by potentiating these effects. A second mutation, substituting proline for histidine 90, was found to cosegregate with a similar clinical syndrome in an ethnically distinct family.

CONCLUSIONS

These findings indicate a role for *DYRK1B* in adipogenesis and glucose homeostasis and associate its altered function with an inherited form of the metabolic syndrome. (Funded by the National Institutes of Health.)

From the Department of Internal Medicine, Yale Cardiovascular Research Center (A.R.K., M.F., G.-W.G., R.S., S.F., J.H., A.M.), Yale Center for Mendelian Genomics (M.C., S.M., R.P.L., A.M.), Department of Genetics (K.K.K., R.P.L., A.M.), and Howard Hughes Medical Institute (R.P.L.), Yale University School of Medicine, New Haven, CT; the Digestive Disease Research Institute, Shariati Hospital (M.F., K.S.-F., R.M.), and Department of Medical Genetics (M.F.), Tehran University of Medical Sciences, Tehran, the Cardiovascular Research Center, Shiraz University of Medical Sciences, Shiraz (M.K., K.S.-F., M.A.B.B.), and Ardabil University of Medical Sciences, Ardabil (A.H., M.B.) — all in Iran. Address reprint requests to Dr. Mani at arya.mani@yale.edu.

Drs. Keramati, Fathzadeh, Go, and Singh contributed equally to this article.

This article was updated on May 15, 2014, at NEJM.org.

N Engl J Med 2014;370:1909-19.
DOI: 10.1056/NEJMoa1301824

Coronary artery disease is the leading cause of death in men and women worldwide.[1,2] A cluster of highly heritable risk factors known as the metabolic syndrome is an increasingly prevalent predisposing factor for coronary artery disease.[3-5] Although substantial progress has been made in the identification of genetic causes of the individual risk factors,[6-11] the underlying genetic factors that unify their association in the metabolic syndrome are not known. We have previously shown in a family with extreme genotypes that single-gene mutations with large effects can occasionally produce features of this syndrome.[12]

The advent of next-generation sequencing has provided an unprecedented opportunity for the identification of rare variants with moderate-to-large effects.[13] One application of this technique is the identification of rare mutations that account for extreme phenotypes in outlier populations. In such populations, the possibility of identifying founder mutations that segregate with extreme phenotypes is dramatically increased.[14-19] We used linkage analysis and whole-exome sequencing to investigate three large families, each of which had a recurring familial pattern of central (or abdominal) obesity associated with early-onset coronary artery disease, severe hypertension, and type 2 diabetes mellitus.

Methods

Study Oversight

The study was conducted in compliance with the provisions of the Declaration of Helsinki.[20] The study protocol was approved by the institutional review board of Shiraz University of Medical Sciences and the ethics committee at Yale University. The adherence of the study to the protocol was monitored by authorities at Shiraz University of Medical Sciences. Written informed consent was obtained from all study participants.

Study Participants

We identified three families (with members of one family not known to be closely related to members of another family) from a community in southwest Iran on the basis of their unusual constellation of juvenile-onset central obesity (Fig. S1 in the Supplementary Appendix, available with the full text of this article at NEJM.org) associated with early-onset coronary artery disease, severe hypertension, type 2 diabetes, and modestly elevated fasting serum triglyceride levels (Fig. 1). These families were considered to be outliers because of the low prevalence of early-onset coronary artery disease and obesity in the local community.[21]

Each family was notable for having many affected members with the same syndrome (Table S1 in the Supplementary Appendix) and other family members who did not have these traits (Table S2 in the Supplementary Appendix). In each family, affected members could trace their descent from a common ancestor. The familial clustering and pattern of inheritance of these clinical features were consistent with the effect of a highly penetrant autosomal dominant trait and suggested that the affected family members might share a common founder mutation.

We evaluated family members individually and obtained detailed clinical and laboratory data, including anthropometric and neurohormonal data, for all available living members of the three families who were older than 30 years of age (for details, see the Supplementary Appendix). We obtained blood samples, and genomic DNA was prepared by means of phenol–chloroform extraction.

Genotyping and Analysis of Linkage

DNA samples from 21 living family members from the three study families were available for genetic studies, including from 14 family members with angiographically diagnosed early-onset coronary artery disease, 5 unaffected family members, and 2 family members with central obesity, hypertension, and diabetes but with unknown status with respect to coronary artery disease. In addition, we collected 2000 DNA samples from ethnically matched controls.

We performed genomewide analysis of linkage using HumanOmni1-Quad BeadChips (Illumina), containing more than 1.1 million single-nucleotide-polymorphism (SNP) markers. After linkage to a segment of chromosome 19q13 was identified, additional markers were typed in selected intervals to generate a dense map of the linked interval. We performed the analysis of linkage using Genehunter 2.1 software. We estimated the allele frequencies on the basis of mean frequencies from a group of 10 ethnically matched controls.

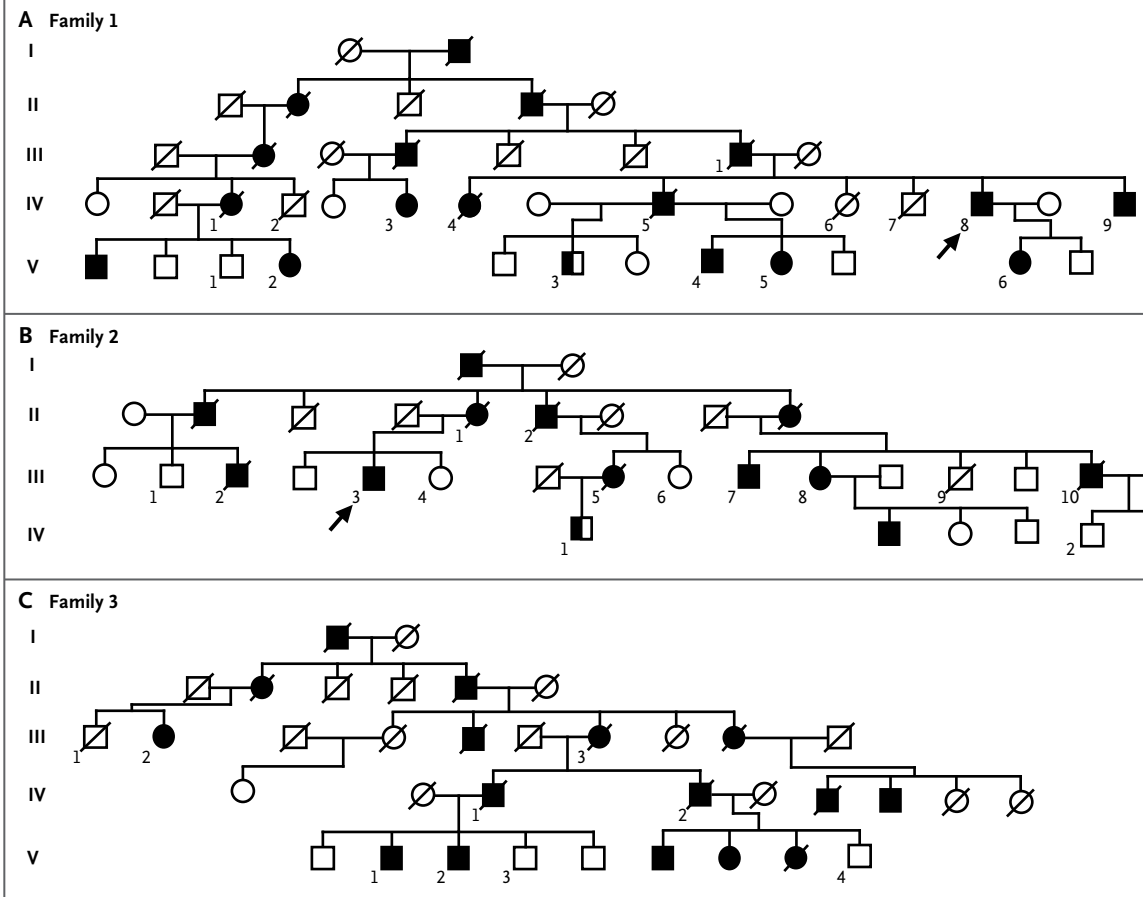

Figure 1. Pedigrees of Three Families with Autosomal Dominant Inheritance of Early-Onset Coronary Artery Disease and Features of the Metabolic Syndrome.

Family members for whom clinical and laboratory data were available for this study are designated by numbers in each generation. Circles indicate female family members, and squares male family members; slashes indicate that the family member is deceased. Family members with early coronary artery disease are indicated by solid symbols, and those without coronary artery disease are indicated by open symbols. All family members with coronary artery disease also had clinical features of the metabolic syndrome (Tables S1 and S2 in the Supplementary Appendix). The index patients (Patient IV-8 in Family 1 and Patient III-3 in Family 2) are indicated by arrows. Two family members with clinical features of the metabolic syndrome but with unknown status with respect to coronary artery disease are indicated by half-solid symbols.

TARGETED SEQUENCE CAPTURE AND SEQUENCING

The index patients from the two largest families were screened for mutations by means of whole-exome sequencing. Genomic DNA was captured on exomes with the use of the Sequence Capture Human Exome 2.1M Array (Roche NimbleGen). The captured libraries were sequenced on the Illumina Genome Analyzer, after which image analysis and base calling were performed. The resulting sequence data were processed with the use of MAQ[22] software. SAMtools software was used to detect single-nucleotide variants. The raw output was further filtered, as described previously, to remove common variants reported in reference genomes.[23] Filters were also applied against published databases. Variants were annotated on the basis of the effect on the protein, novelty, conservation, and tissue expression with the use of an automated pipeline for genome annotation.[19]

A novel variant was identified in *DYRK1B*, the gene encoding dual-specificity tyrosine-phosphorylation-regulated kinase 1B. In this variant, cysteine is substituted for arginine at position 102 in *DYRK1B* (Fig. S2 in the Supplementary Appendix).

FUNCTIONAL ANALYSIS OF *DYRK1B* R102C

We examined the effects of expression of nonmutated DYRK1B and the novel variant DYRK1B R102C, as well as the effects of DYRK1B knockdown using short hairpin RNA (shRNA), on adipogenic differentiation in permanent 3T3-L1 preadipocyte cell lines. We also examined the effects of DYRK1B variants on the expression of glucose-6-phosphatase in HepG2 cells. Details of the functional analyses are provided in the Methods section in the Supplementary Appendix.

STATISTICAL ANALYSIS

We performed all in vitro experiments in groups of four. Data are expressed as means and standard errors. We used the Mann–Whitney U test to perform between-group comparisons (two-tailed). For multiple comparisons, we performed Tukey's test in conjunction with analysis of variance using GraphPad Prism software. We used analysis of variance to compare the metabolic traits with adjustment and without adjustment for age and sex as covariates. A P value of less than 0.05 was considered to indicate statistical significance. All P values are two-sided.

RESULTS

STUDY POPULATION

The clinically characterized members of the three study families included 25 affected family members (Table S1 in the Supplementary Appendix), 12 unaffected family members (Table S2 in the Supplementary Appendix), and 2 family members with clinical features of the metabolic syndrome but with unknown status with respect to coronary artery disease (Table S1 in the Supplementary Appendix). All 25 affected family members had early-onset myocardial infarction or coronary artery disease at a mean (±SE) age of 44.8±2.6 years in men and 44.2±1.8 years in women. Additional clinical features included central obesity (Table S3 in the Supplementary Appendix), type 2 diabetes, and hypertension; the presence of all three conditions was not explained by neurohormonal activation (Table S4 in the Supplementary Appendix). The constellation of medical conditions in all the affected family members (and none of the unaffected family members) met the standard definition of the metabolic syndrome, according to the criteria of the National Cholesterol Education Program of the National Institutes of Health.[24]

LINKAGE ANALYSIS

We performed a genomewide multipoint parametric analysis of linkage, using samples obtained from affected family members and specifying coronary artery disease as an autosomal dominant trait. Each family was analyzed independently. Two different prespecified models of the trait locus were applied, with disease allele frequencies of 10^{-4} and 10^{-5} and phenocopy rates of 0.001 and 0.0001, respectively. Under the two models, the analysis showed significant evidence of linkage of coronary artery disease to a small segment of chromosome 19q13. Under the stringent model, the maximum multipoint logarithm of odds (LOD) score was 5.27 in the analysis of affected family members (Fig. 2A) and 6.34 (odds ratio, 2,187,761:1 in favor of linkage) after the inclusion of unaffected family members in the analysis. All three families had LOD scores close to the theoretical maximum. No other interval showed a multipoint LOD score greater than 1.0. Separate linkage analyses of the 19q13 region with central obesity, hypertension, and type 2 diabetes showed similar results (Fig. 2A).

Scrutiny of the linked haplotypes showed that all three families shared identical markers spanning a 6.1-Mbp haplotype flanked by the markers rs833917 and rs4801770 (Fig. 2B). Haplotype sharing among the families was indicative of their common ancestral origin and suggested the presence of a founder mutation (Fig. S3 in the Supplementary Appendix). No family member was homozygous for this haplotype.

WHOLE-EXOME SEQUENCING

We filtered data from whole-exome sequencing in the two index patients by removing common SNPs. We excluded variants that were found in the NHLBI ESP5400 exome database and the Yale Center for Genome Analysis exome database, and we identified rare protein-altering variants in each family member. Among these variants, only 18 rare variants were shared by the two index patients (Table S5 in the Supplementary Appendix), and only 1 was found in the linkage interval on chromosome 19. Genotyping resulted in complete cosegregation of this variant with coronary artery disease in all three families.

The mutation substituted cysteine for arginine at position 102 of *DYRK1B* (Fig. 2C). None of the other 17 variants were found in more than five of the affected members, and some were

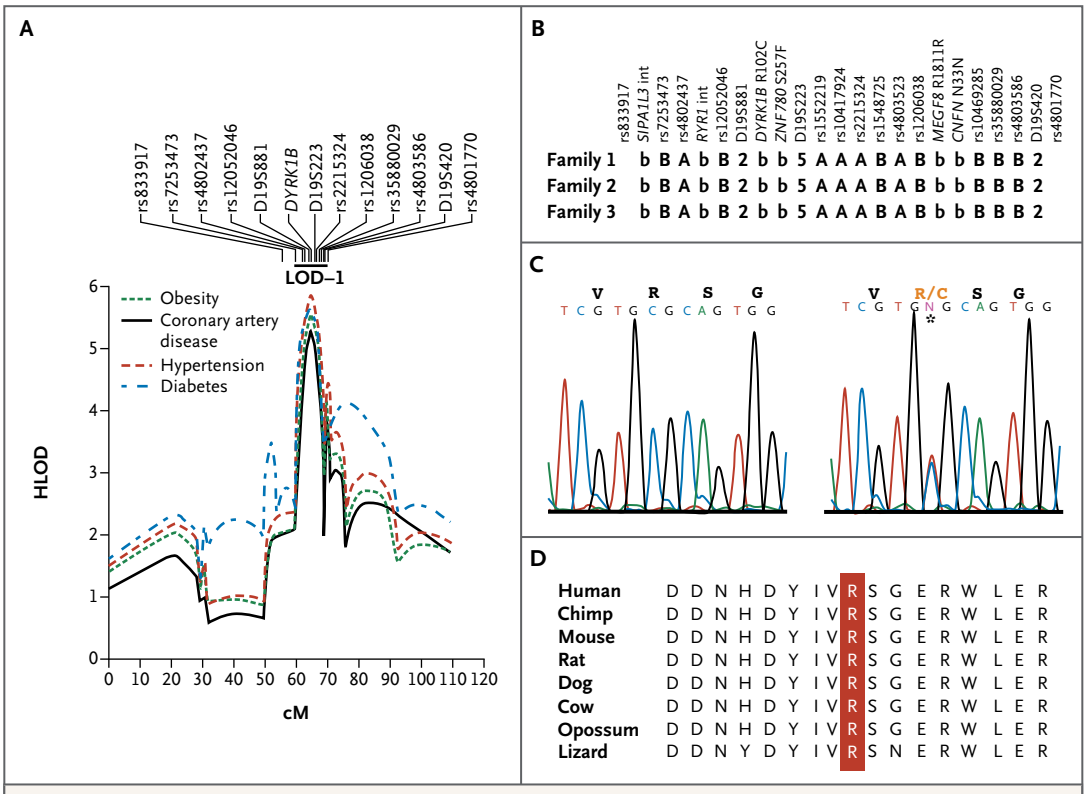

Figure 2. Identification of a *DYRK1B* Mutation Cosegregating with the Metabolic Syndrome in the Three Study Families.

Panel A shows multipoint heterogeneity LOD (HLOD) scores for linkage of early coronary artery disease, obesity, type 2 diabetes, and high blood pressure to chromosome 19q13. Shown are single-nucleotide polymorphisms and microsatellites (short tandem repeats of two to five nucleotides) that are tightly linked to the location of *DYRK1B* in the LOD–1 support interval (in which the LOD score is greater than or equal to the maximum minus 1.0, as measured in centimorgans [cM]). The peak of the LOD score occurs at zero recombination with marker D19S881, and the LOD–1 support interval spans 6 cM for all four traits. Panel B shows the minimum shared haplotypes of the three affected families. Listed are two nonsense mutations (*DYRK1B* R102C and *ZNF780* S257F), two intronic (int) mutations, and two synonymous mutations (*MEGF8* R1811R and *CNFN* N33N) that were shared by affected family members within the shared haplotype. The only novel mutation was *DYRK1B* R102C. The uppercase and lowercase letters in bold below the mutations and SNPs indicate major and minor alleles, respectively, and the numbers below the microsatellites in bold indicate arbitrary allele numbers. Panel C shows the DNA sequence of a segment flanking R102 in *DYRK1B* from an unaffected family member (at left) and a heterozygous mutation carrier (at right). A single base substitution (indicated by an asterisk) changes the nonmutant cytosine to thymine, leading to the substitution of cysteine (C) for arginine (R) at codon 102. N denotes a heterozygote C→T nucleotide substitution. Panel D shows a portion of the amino acid sequence of DYRK1B from diverse vertebrate species. This segment is highly conserved, and arginine 102 is completely conserved in orthologues in species ranging from lizards to humans.

also found in unaffected family members (Table S5 in the Supplementary Appendix).

The arginine residue at position 102 of *DYRK1B* is found in a kinase-like domain of the protein (Fig. S2 in the Supplementary Appendix) and is highly conserved among orthologues and paralogues in species ranging from lizards to humans (Fig. 2D). The R102C mutation was absent in chromosome samples obtained from 2000 ethnically matched Iranians and 3600 white controls in the United States. The mutation was also absent in samples obtained from 2500 persons of diverse ethnic backgrounds in the Allele Frequency Database (ALFRED) (Table S6 in the Supplementary Appendix), 5000 exomes from the Yale Center for Genome Analysis database, and 5400 exomes in the NHLBI ESP5400 database. Both the PolyPhen-1 and PolyPhen-2 poly-

morphism-phenotyping programs predicted the variant to be deleterious.

We performed parametric analysis of linkage in affected family members using body-mass index, blood pressure, or type 2 diabetes as the phenotype. This analysis confirmed linkage to the *DYRK1B* R102C mutation, with LOD scores of 5.63, 5.86, and 5.70 for the three variables, respectively. After adjustment for age and sex, differences in fasting blood glucose levels, blood-pressure levels, and body-mass index between mutation carriers and noncarriers were highly significant (Table 1). There was a trend toward higher levels of serum low-density lipoprotein cholesterol and triglycerides in mutation carriers, as compared with noncarriers.

EFFECT OF *DYRK1B* R102C ON ADIPOGENIC TRANSFORMATION

DYRK1B belongs to the Dyrk family of proteins, a group of evolutionarily conserved protein kinases that are involved in cell differentiation, survival, and proliferation.[25-27] The DYRK1B protein is an arginine-directed serine–threonine kinase, which is ubiquitously expressed in mice[28] and humans (see the Methods section and Fig. S4 in the Supplementary Appendix).

The expression of DYRK1B increases dramatically during adipogenic differentiation.[28] Adipogenesis is a process of maturation of undifferentiated mesenchymal stem cells toward the adipocyte lineage. The inhibition of sonic hedgehog (SHH) pathways results in decreased expression of Wnt proteins[29] and is associated with increased expression of the adipogenic proteins CCAAT/enhancer-binding protein α (C/EBPα) and peroxisome proliferator-activated receptor γ (PPARγ)[30] and adipogenic transformation.[31] Since DYRK1B inhibits SHH signaling,[32] we hypothesized that it promotes adipogenesis.

We examined the effects of nonmutant DYRK1B, DYRK1B R102C, and knockdown of DYRK1B on adipogenic differentiation in 3T3-L1 cells. An adipogenic medium that contains the Wnt inhibitor IBMX was used to stimulate differentiation of the 3T3-L1 cells into adipocytes. We examined the expression of C/EBPα and PPARγ isoforms 1 and 2, along with the expression of Gli-2 (a mediator of Shh signaling), PGC1α (a transcriptional coactivator that interacts with PPARγ), and cyclin-dependent kinase inhibitor (p27Kip), which is regulated by DYRK1B and is involved in adipogenic differentiation.[33,34]

Total levels of DYRK1B expression were similar in cells expressing either nonmutant DYRK1B or DYRK1B R102C (Fig. S5 in the Supplementary Appendix). Adipogenic differentiation (as shown by means of oil red O staining) started approximately 5 days earlier in cells expressing nonmutant DYRK1B or DYRK1B R102C than in those transfected with vector alone, and the accumulation of intracellular lipid (as judged by the inten-

Table 1. Comparison of Metabolic Traits in *DYRK1B* R102C Carriers and Noncarriers in the Three Study Families.*

Trait	Nonmutated *DYRK1B*	*DYRK1B* R102C	P Value	
			Unadjusted	Adjusted†
Fasting blood glucose (mg/dl)	94.6±1.7	175.8±12.5	0.001	0.003
Low-density lipoprotein cholesterol (mg/dl)	84.0±10.6	109.1±9.8	0.17	0.09
Triglycerides (mg/dl)	111.4±12.2	168.1±16.9	0.07	0.09
Blood pressure (mm Hg)				
Systolic	110.0±4.4	175.3±5.5	<0.001	<0.001
Diastolic	78.0±2.6	99.5±2.2	<0.001	<0.001
Body-mass index‡	23.6±0.5	33.0±0.4	<0.001	<0.001

* Plus–minus values are means ±SE. Included in this analysis were 16 affected family members (including 2 with clinical features of the metabolic syndrome but with unknown status with respect to coronary artery disease) and 5 unaffected family members for whom genotype data were available. All analyses were performed with the use of analysis of variance. To convert the values for glucose to millimoles per liter, multiply by 0.05551. To convert the values for cholesterol to millimoles per liter, multiply by 0.02586. To convert the values for triglycerides to millimoles per liter, multiply by 0.01129.

† P values were adjusted for age and sex.

‡ The body-mass index is the weight in kilograms divided by the square of the height in meters.

sity of staining) was significantly greater in cells expressing DYRK1B R102C than in cells expressing nonmutant DYRK1B or in cells transfected with vector alone (Fig. 3A). Accordingly, the expression levels of C/EBPα, PPARγ isoforms 1 and 2, and PGC1α were highest, and those of Gli-2 and p27Kip were lowest, in cells expressing the R102C variant, followed by cells expressing the nonmutant form of the protein and those transfected with empty vector (Fig. 3B, and Fig. S6 in the Supplementary Appendix). DYRK1B knockdown diminished the expression of C/EBPα, PPARγ isoforms 1 and 2, and PGC1α and abrogated adipocyte differentiation (Fig. 3A and 3C).

The effect of nonmutant DYRK1B and the R102C variant on Wnt signaling was examined in a well-established dual luciferase reporter assay,[35,36] with and without Wnt3a stimulation. Wnt signaling activity was lowest in cells expressing the R102C variant, followed by cells expressing the nonmutant form, and was highest in cells transfected with empty vector (Fig. S7 in the Supplementary Appendix). Correspondingly, cells expressing the R102C variant were able to transform into mature adipocytes without requiring the addition of the adipogenic medium (Fig. 3D).

EFFECT OF R102C VARIANT ON GLUCOSE-6-PHOSPHATASE

Another function of DYRK1B is the induction of the key gluconeogenic enzyme glucose-6-phosphatase.[37] Increased expression[38,39] and activity[40] of glucose-6-phosphatase are associated with elevated fasting glucose levels in patients with type 2 diabetes.[41] In a luciferase reporter assay, DYRK1B R102C significantly potentiated the induction of glucose-6-phosphatase (Fig. 4A). This finding was confirmed by the increased expression of glucose-6-phosphatase messenger RNA and protein in cells expressing the R102C variant, as compared with cells expressing the nonmutant protein and cells transfected with vector alone (Fig. 4B and 4C, and Fig. S8 in the Supplementary Appendix). The analysis further showed that DYRK1B-associated induction of glucose-6-phosphatase is dose-dependent (Fig. 4D, and Fig. S8 in the Supplementary Appendix), which confirms a gain-of-function effect of the R102C variant. This function of DYRK1B is independent of its kinase activity, since the kinase-defective mutant DYRK1B Y271/273F and the nonmutant protein showed similar effects on glucose-6-phosphatase expression (Fig. 4C, and Fig. S8 in the Supplementary Appendix).

ASSOCIATION BETWEEN A SECOND *DYRK1B* ALLELE AND CENTRAL OBESITY AND DIABETES

We screened 300 morbidly obese white patients with coronary artery disease and multiple metabolic phenotypes for the *DYRK1B* R102C allele. This led to the identification of a novel *DYRK1B* allele (H90P) in five unrelated patients. We then evaluated DNA samples obtained from family members of one of the mutation carriers, which showed a consistent pattern of cosegregation of the novel allele with features of the metabolic syndrome in an autosomal dominant pattern. In vitro studies showed that the presence of *DYRK1B* H90P enhanced glucose-6-phosphatase expression. (See the Methods section and Fig. S8C and S9 in the Supplementary Appendix.)

DISCUSSION

Our study establishes an association between mutations in *DYRK1B* and a syndrome of central obesity, early-onset coronary artery disease, hypertension, and type 2 diabetes. Our evidence includes the finding of an identical nonconservative mutation on a shared haplotype background in three separate families with this syndrome, the identification of a second nonconservative mutation in an ethnically distinct population with a similar phenotype, and biochemical data indicating that the mutations alter two important functions of the encoded protein. These results show that rare alleles may underlie an association with a cluster of metabolic risk factors of coronary artery disease known as the metabolic syndrome.

The *DYRK1B* locus on 19q13 has been linked to type 2 diabetes[42,43] and traits associated with the metabolic syndrome[44] in genomewide association studies. This raises the question of whether common genetic variants in *DYRK1B* are also associated with these traits in the general population. Most if not all carriers of the *DYRK1B* R102C and H90P mutations were obese, had hypertension and diabetes, and met the criteria for the metabolic syndrome. These observations indicate the broad and important effect of the mutated gene and suggest that the clustering of the individual risk factors imparts extremely high cardiovascular risk to mutation carriers.

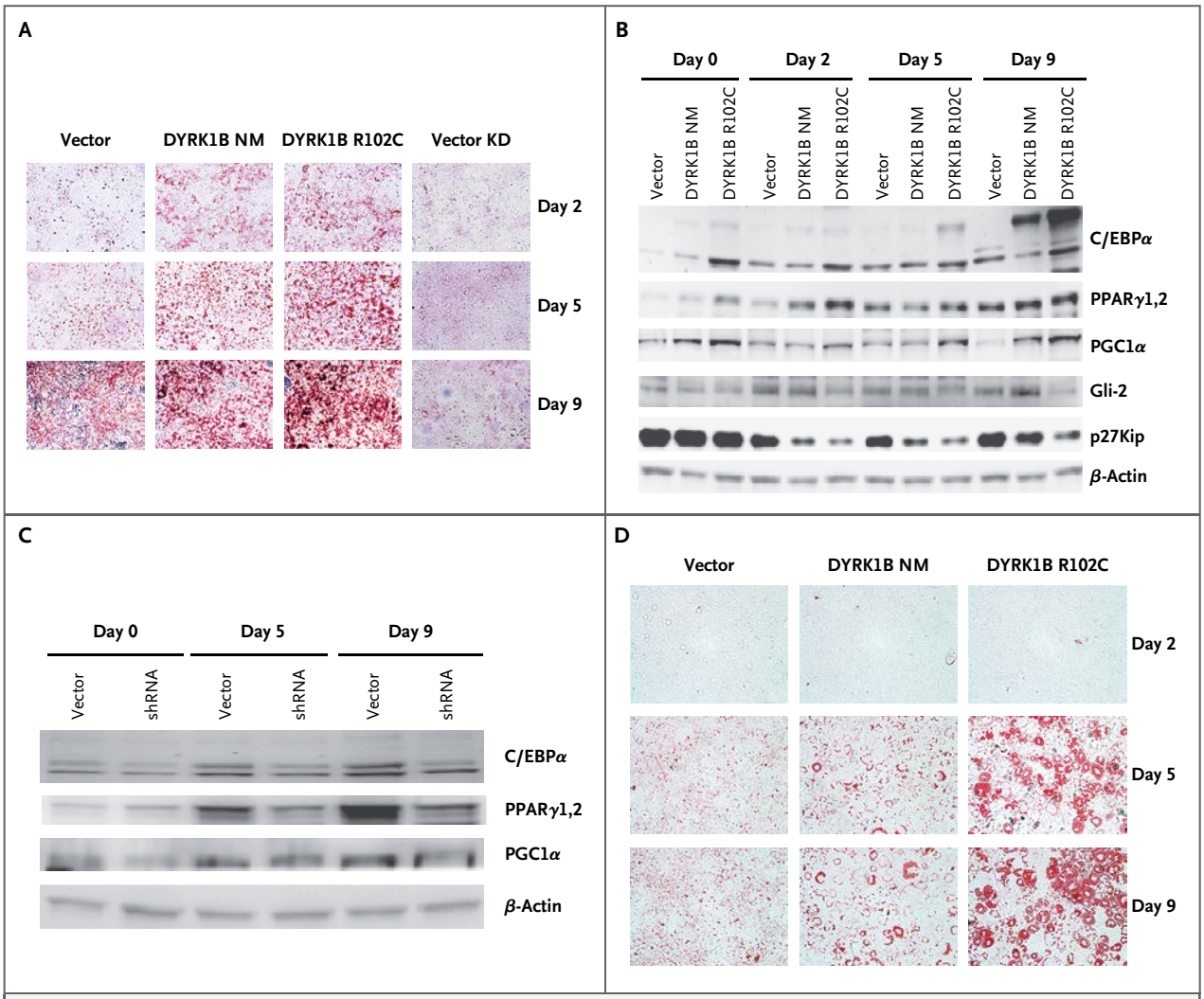

Figure 3. Enhanced Adipogenic Effect Associated with *DYRK1B* R102C.

Permanent 3T3-L1 preadipocyte cell lines expressing nonmutant DYRK1B, the DYRK1B R102C mutation, DYRK1B-specific short hairpin RNA (shRNA), or vector alone were created, and the time course of adipocyte differentiation was examined. Panel A shows adipogenic transformations for days 2, 5, and 9. Staining with oil red O shows the presence of intracellular lipid, thus labeling adipocytes. Cells expressing nonmutant (NM) DYRK1B or DYRK1B R102C were transformed into adipocytes considerably earlier than were cells transfected with an empty vector. The accumulation of intracellular lipid (as judged by the intensity of staining) was highest in cells expressing DYRK1B R102C, followed by those expressing nonmutant DYRK1B, and lowest in cells transfected with an empty vector. No significant adipogenic differentiation was observed in cells expressing DYRK1B-specific shRNA (DYRK1B knockdown [KD]). Panel B shows the expression levels of CCAAT/enhancer-binding protein α (C/EBPα), peroxisome proliferator-activated receptor γ (PPARγ) isoforms 1 and 2, and PGC1α (a transcriptional coactivator that interacts with PPARγ), which were highest in adipocytes expressing the R102C variant, followed by those expressing nonmutant DYRK1B, and lowest in cells transfected with vector alone from early stages of adipogenesis. Conversely, the expression levels of Gli-2 (a mediator of sonic hedgehog signaling) and cyclin-dependent kinase inhibitor (p27Kip) were lowest in adipocytes expressing the R102C variant, followed by cells expressing nonmutant DYRK1B, and highest in those transfected with vector alone. β-actin was used as a loading control. Panel C shows that the expression levels of C/EBPα, PPARγ isoforms 1 and 2, and PGC1α were significantly lower in DYRK1B knockdown cells than in cells transfected with vector alone. Panel D shows that cells expressing the R102C variant had substantial adipogenic transformation without the addition of adipogenic medium, as compared with those expressing nonmutant DYRK1B or those transfected with vector alone.

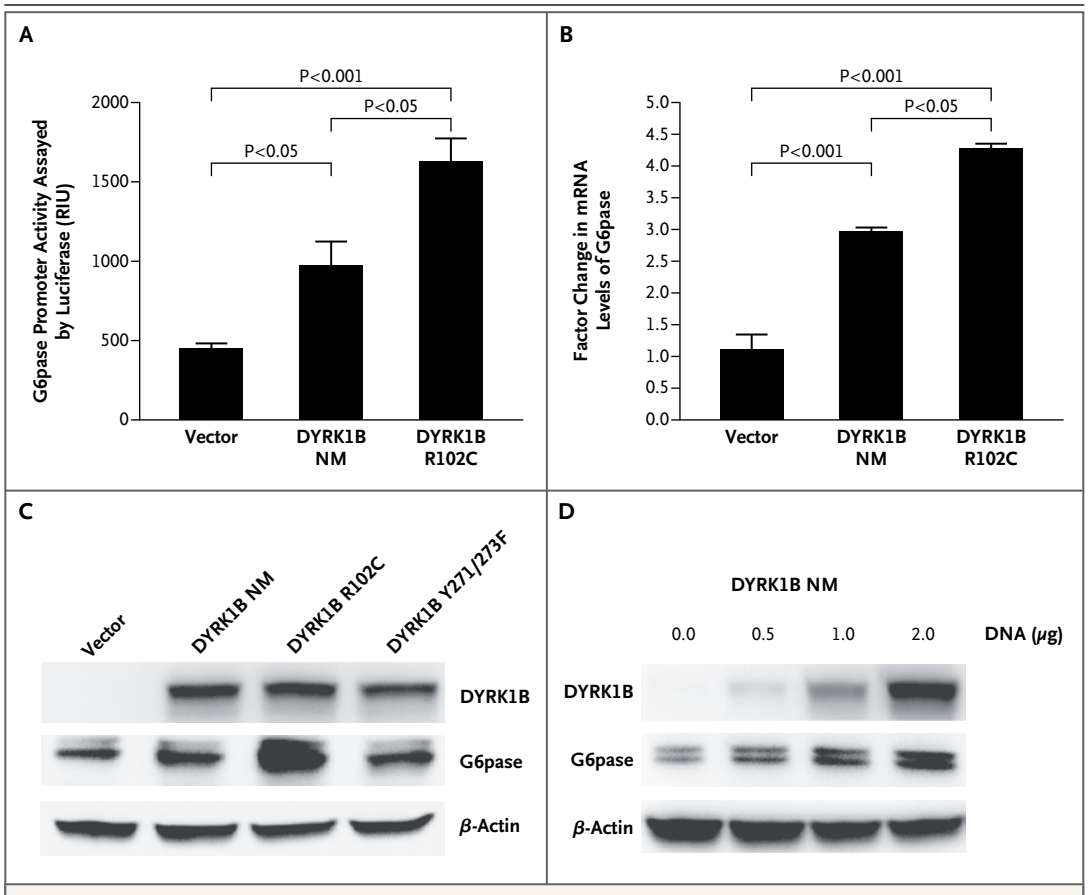

Figure 4. Enhanced Kinase-Independent Induction of Glucose-6-Phosphatase by *DYRK1B* R102C.

Panel A shows nonmutant DYRK1B and DYRK1B R102C expressed in HepG2 cells. Their transcriptional activities were assayed by glucose-6-phosphatase (G6pase) promoter-mediated expression of luciferase, as measured in refractive index units (RIU). Nonmutant DYRK1B more than doubled the activity of luciferase, as compared with vector alone. The effect of DYRK1B R102C on luciferase activity was more than 1.5 times the effect of nonmutant DYRK1B. The T bars indicate standard errors. Panel B shows that the messenger RNA expression levels of glucose-6-phosphatase were significantly higher in cells expressing DYRK1B R102C than in those expressing nonmutant DYRK1B or vector alone. Panel C shows nonmutant DYRK1B, the R102C variant, and the kinase-defective mutant DYRK1B Y271/273F expressed in HepG2 cells. Their effect on glucose-6-phosphatase expression was assayed with the use of Western blotting. The protein expression level of glucose-6-phosphatase was highest in cells expressing the R102C variant. The next highest levels were in cells expressing nonmutant (NM) DYRK1B and the kinase-defective Y271/273F variant, which were roughly equal and significantly higher than in the vector alone. Panel D shows the dose effect of nonmutant DYRK1B on endogenous glucose-6-phosphatase expression.

Very little is known about the function of DYRK1B and its role in human disease. DYRK1B is a nutrient-sensing protein that inhibits the RAS–RAF–MEK pathway,[45] which is widely recognized for its regulation of glucose uptake and glycolysis.[46] Mice that are deficient in kinase suppressor of ras 2 (KSR2), the molecular scaffold of RAS–RAF–MEK, are obese and have insulin resistance.[47] Loss-of-function mutations in *KSR2* have been shown to be associated with childhood obesity and insulin resistance.[48] These mutations similarly impair the RAS–RAF–MEK pathway, a finding that is consistent with the gain-of-function effects of *DYRK1B* mutations.

The increased expression of DYRK1B during adipogenic differentiation[28] is suggestive of its

involvement in adipogenesis. DYRK1B may enhance adipogenesis through inhibition of the SHH pathway or by increasing the turnover of p27Kip.[33,34,49] Mice that are deficient in p27Kip are observed to have atherosclerosis,[50-52] obesity, and insulin resistance.[53] In our study, we found that the *DYRK1B* R102C mutation augments p27Kip turnover and potentiates the adipogenic effects of DYRK1B. Our findings are consistent with the recent observation that the overexpression of DYRK1B homologue DYRK1A and minibrain protein in mice and drosophila leads to an increase in food intake and body weight, and deficiencies are associated with loss of body weight.[54]

Previous studies have also shown that DYRK1B promotes in vitro transcription of the key hepatic gluconeogenic enzyme glucose-6-phosphatase.[41] We found that this function of DYRK1B is kinase-independent and is augmented by the *DYRK1B* R102C and H90P mutations. These in vitro studies provide initial insights into some of the potential disease mechanisms through which *DYRK1B* mutations may contribute to the metabolic syndrome.

In conclusion, we found that mutations in *DYRK1B* are associated with a clinical phenotype that is characterized by central obesity, hypertension, type 2 diabetes, and early-onset coronary artery disease. Our findings suggest that DYRK1B plays a central role in the biologic pathways that are disrupted in the disorder known as the metabolic syndrome.

Supported by grants from the National Institutes of Health (NIH) (R01HL094784-01 and R01HL094574-03, to Dr. Mani) and by a grant from the NIH Centers for Mendelian Genomics (5U54HG006504).

No potential conflict of interest relevant to this article was reported.

Disclosure forms provided by the authors are available with the full text of this article at NEJM.org.

We thank Reza Mohammadi and Tahmures Mohammadi, local schoolteachers, and Dr. Mohammad Javad Zibaee Nezhad, director of the Cardiovascular Research Center, Shiraz University of Medical Sciences, for their active role in identification and recruitment of the family members; Dr. Javad Tavakkoly Bazzaz, head of the Department of Medical Genetics, Tehran University of Medical Sciences, and Saeed Pour Ali, deputy for research, Iranian Academic Center for Education, Culture, and Research, for their organizational support for patient recruitment; Dr. Sekar Kathiresan at the Massachusetts General Hospital and Drs. Orhan Buglivar and Murat Gunel at the Yale University School of Medicine for providing us with access to their whole-exome-sequencing database; and Dr. Nicholas Gekakis at the Scripps Institute for providing us with glucose-6-phosphatase–responsive luciferase plasmid.

REFERENCES

1. Katakura M, Naka M, Kondo T, et al. Prospective analysis of mortality, morbidity, and risk factors in elderly diabetic subjects: Nagano study. Diabetes Care 2003;26:638-44.
2. Beaglehole R. International trends in coronary heart disease mortality, morbidity, and risk factors. Epidemiol Rev 1990; 12:1-15.
3. Rathmann W, Giani G. Global prevalence of diabetes: estimates for the year 2000 and projections for 2030. Diabetes Care 2004;27:2568-9.
4. Boyle JP, Honeycutt AA, Narayan KM, et al. Projection of diabetes burden through 2050: impact of changing demography and disease prevalence in the U.S. Diabetes Care 2001;24:1936-40.
5. Mokdad AH, Ford ES, Bowman BA, et al. Prevalence of obesity, diabetes, and obesity-related health risk factors, 2001. JAMA 2003;289:76-9.
6. Hobbs HH, Russell DW, Brown MS, Goldstein JL. The LDL receptor locus in familial hypercholesterolemia: mutational analysis of a membrane protein. Annu Rev Genet 1990;24:133-70.
7. Hobbs HH, Brown MS, Goldstein JL. Molecular genetics of the LDL receptor gene in familial hypercholesterolemia. Hum Mutat 1992;1:445-66.
8. Goldstein JL, Brown MS. Familial hypercholesterolemia: identification of a defect in the regulation of 3-hydroxy-3-methylglutaryl coenzyme A reductase activity associated with overproduction of cholesterol. Proc Natl Acad Sci U S A 1973;70:2804-8.
9. Ahlqvist E, Ahluwalia TS, Groop L. Genetics of type 2 diabetes. Clin Chem 2011;57:241-54.
10. Bonnefond A, Froguel P, Vaxillaire M. The emerging genetics of type 2 diabetes. Trends Mol Med 2010;16:407-16.
11. Lifton RP, Gharavi AG, Geller DS. Molecular mechanisms of human hypertension. Cell 2001;104:545-56.
12. Mani A, Radhakrishnan J, Wang H, et al. LRP6 mutation in a family with early coronary disease and metabolic risk factors. Science 2007;315:1278-82. [Erratum, Science 2013;341:959.]
13. Teer JK, Mullikin JC. Exome sequencing: the sweet spot before whole genomes. Hum Mol Genet 2010;19:R145-R151.
14. Agrawal N, Frederick MJ, Pickering CR, et al. Exome sequencing of head and neck squamous cell carcinoma reveals inactivating mutations in NOTCH1. Science 2011;333:1154-7.
15. Tiacci E, Trifonov V, Schiavoni G, et al. *BRAF* mutations in hairy-cell leukemia. N Engl J Med 2011;364:2305-15.
16. Barak T, Kwan KY, Louvi A, et al. Recessive LAMC3 mutations cause malformations of occipital cortical development. Nat Genet 2011;43:590-4.
17. DePristo MA, Banks E, Poplin R, et al. A framework for variation discovery and genotyping using next-generation DNA sequencing data. Nat Genet 2011;43:491-8.
18. Wei X, Walia V, Lin JC, et al. Exome sequencing identifies GRIN2A as frequently mutated in melanoma. Nat Genet 2011;43:442-6.
19. Choi M, Scholl UI, Ji W, et al. Genetic diagnosis by whole exome capture and massively parallel DNA sequencing. Proc Natl Acad Sci U S A 2009;106:19096-101.
20. Declaration of Helsinki: ethical principles for medical research involving human subjects. Ferney-Voltaire, France: World Medical Association, 2006.
21. Pishdad GR. Overweight and obesity in adults aged 20-74 in southern Iran. Int J Obes Relat Metab Disord 1996;20:963-5.
22. Li H, Ruan J, Durbin R. Mapping short DNA sequencing reads and calling variants using mapping quality scores. Genome Res 2008;18:1851-8.
23. Ng PC, Levy S, Huang J, et al. Genetic variation in an individual human exome. PLoS Genet 2008;4(8):e1000160.
24. Alexander CM, Landsman PB, Grundy SM. The influence of age and body mass index on the metabolic syndrome and its

components. Diabetes Obes Metab 2008; 10:246-50.
25. Tejedor F, Zhu XR, Kaltenbach E, et al. *minibrain*: A new protein kinase family involved in postembryonic neurogenesis in Drosophila. Neuron 1995;14:287-301.
26. Lee K, Deng X, Friedman E. Mirk protein kinase is a mitogen-activated protein kinase substrate that mediates survival of colon cancer cells. Cancer Res 2000;60: 3631-7.
27. Yang EJ, Ahn YS, Chung KC. Protein kinase Dyrk1 activates cAMP response element-binding protein during neuronal differentiation in hippocampal progenitor cells. J Biol Chem 2001;276:39819-24.
28. Leder S, Czajkowska H, Maenz B, et al. Alternative splicing variants of dual specificity tyrosine phosphorylated and regulated kinase 1B exhibit distinct patterns of expression and functional properties. Biochem J 2003;372:881-8.
29. Borycki A, Brown AM, Emerson CP Jr. Shh and Wnt signaling pathways converge to control Gli gene activation in avian somites. Development 2000;127: 2075-87.
30. Ross SE, Hemati N, Longo KA, et al. Inhibition of adipogenesis by Wnt signaling. Science 2000;289:950-3.
31. Suh JM, Gao X, McKay J, McKay R, Salo Z, Graff JM. Hedgehog signaling plays a conserved role in inhibiting fat formation. Cell Metab 2006;3:25-34.
32. Lauth M, Bergström A, Shimokawa T, et al. DYRK1B-dependent autocrine-to-paracrine shift of Hedgehog signaling by mutant RAS. Nat Struct Mol Biol 2010; 17:718-25.
33. Tang QQ, Otto TC, Lane MD. CCAAT/enhancer-binding protein beta is required for mitotic clonal expansion during adipogenesis. Proc Natl Acad Sci U S A 2003;100:850-5.
34. Tang QQ, Otto TC, Lane MD. Mitotic clonal expansion: a synchronous process required for adipogenesis. Proc Natl Acad Sci U S A 2003;100:44-9.
35. Boyden LM, Mao J, Belsky J, et al. High bone density due to a mutation in LDL-receptor-related protein 5. N Engl J Med 2002;346:1513-21.
36. Mao J, Wang J, Liu B, et al. Low-density lipoprotein receptor–related protein-5 binds to Axin and regulates the canonical Wnt signaling pathway. Mol Cell 2001; 7:801-9.
37. von Groote-Bidlingmaier F, Schmoll D, Orth HM, Joost HG, Becker W, Barthel A. DYRK1 is a co-activator of FKHR (FOXO1a)-dependent glucose-6-phosphatase gene expression. Biochem Biophys Res Commun 2003;300:764-9.
38. Argaud D, Zhang Q, Pan W, Maitra S, Pilkis SJ, Lange AJ. Regulation of rat liver glucose-6-phosphatase gene expression in different nutritional and hormonal states: gene structure and 5′-flanking sequence. Diabetes 1996;45:1563-71.
39. Liu Z, Barrett EJ, Dalkin AC, Zwart AD, Chou JY. Effect of acute diabetes on rat hepatic glucose-6-phosphatase activity and its messenger RNA level. Biochem Biophys Res Commun 1994;205: 680-6.
40. Segal HL, Washko ME. Studies of liver glucose 6-phosphatase. III. Solubilization and properties of the enzyme from normal and diabetic rats. J Biol Chem 1959;234:1937-41.
41. Altomonte J, Richter A, Harbaran S, et al. Inhibition of Foxo1 function is associated with improved fasting glycemia in diabetic mice. Am J Physiol Endocrinol Metab 2003;285(4):E718-E728.
42. Sim X, Ong RT, Suo C, et al. Transferability of type 2 diabetes implicated loci in multi-ethnic cohorts from Southeast Asia. PLoS Genet 2011;7(4):e1001363.
43. Cho YS, Chen CH, Hu C, et al. Meta-analysis of genome-wide association studies identifies eight new loci for type 2 diabetes in east Asians. Nat Genet 2012; 44:67-72.
44. Kraja AT, Vaidya D, Pankow JS, et al. A bivariate genome-wide approach to metabolic syndrome: STAMPEED consortium. Diabetes 2011;60:1329-39.
45. Friedman E. Mirk/dyrk1B Kinase in ovarian cancer. Int J Mol Sci 2013;14:5560-75.
46. Yun J, Rago C, Cheong I, et al. Glucose deprivation contributes to the development of KRAS pathway mutations in tumor cells. Science 2009;325:1555-9.
47. Costanzo-Garvey DL, Pfluger PT, Dougherty MK, et al. KSR2 is an essential regulator of AMP kinase, energy expenditure, and insulin sensitivity. Cell Metab 2009;10:366-78.
48. Pearce LR, Atanassova N, Banton MC, et al. *KSR2* mutations are associated with obesity, insulin resistance, and impaired cellular fuel oxidation. Cell 2013;155:765-77.
49. Ewton DZ, Lee K, Deng X, Lim S, Friedman E. Rapid turnover of cell-cycle regulators found in Mirk/dyrk1B transfectants. Int J Cancer 2003;103:21-8.
50. Díez-Juan A, Andrés V. The growth suppressor p27(Kip1) protects against diet-induced atherosclerosis. FASEB J 2001; 15:1989-95.
51. Akyürek LM, Boehm M, Olive M, Zhou AX, San H, Nabel EG. Deficiency of cyclin-dependent kinase inhibitors p21Cip1 and p27Kip1 accelerates atherogenesis in apolipoprotein E-deficient mice. Biochem Biophys Res Commun 2010;396:359-63.
52. Tanner FC, Yang ZY, Duckers E, Gordon D, Nabel GJ, Nabel EG. Expression of cyclin-dependent kinase inhibitors in vascular disease. Circ Res 1998;82:396-403.
53. Naaz A, Holsberger DR, Iwamoto GA, Nelson A, Kiyokawa H, Cooke PS. Loss of cyclin-dependent kinase inhibitors produces adipocyte hyperplasia and obesity. FASEB J 2004;18:1925-7.
54. Hong SH, Lee KS, Kwak SJ, et al. Minibrain/Dyrk1a regulates food intake through the Sir2-FOXO-sNPF/NPY pathway in Drosophila and mammals. PLoS Genet 2012;8(8):e1002857.